First publ. in: Chemical Physics Letters 396 (2004), 4-6, pp. 341-345

Experimental and theoretical studies on inorganic magic clusters: M_4X_6 (M = W, Mo, X = O, S)

N. Bertram [a], Y.D. Kim [a,*], G. Ganteför [a], Q. Sun [b], P. Jena [b], J. Tamuliene [c], G. Seifert [c]

[a] Department of Physics, University of Konstanz, Universitaetsstrasse 10, D-78457 Konstanz, Germany
[b] Physics Department, Virginia Commonwealth University, Richmond, VA 23284, USA
[c] Institute of Physical Chemistry and Electrochemistry, Technical University Dresden, D-01062 Dresden, Germany

Abstract

Studies using ultraviolet photoelectron spectroscopy (UPS) and density functional theory (DFT) demonstrate that M_4X_6 (M = W, Mo and X = O, S) clusters show large gaps (about 2 eV) between the highest occupied molecular orbital (HOMO) and the lowest unoccupied molecular orbital (LUMO), indicative of their high stability and chemical inertness. In particular, W_4O_6 has a lower symmetry and a larger HOMO–LUMO gap than other hitherto discovered magic clusters. Although the similarity between the electronic structures of W_4O_6 and Mo_4S_6 may be regarded as an indication that both clusters have similar geometric structures, our detailed DFT-calculations reveal otherwise. This result implies that synergetic approach using theoretical and experimental methods are essential to shed light on cluster geometries.

Geometric, electronic and chemical properties of nanostructures are often much different compared to their bulk counterparts. Among various nanoclusters, the interest on so-called 'magic clusters' has been increasing since the discovery of C_{60} [1]. Magic clusters exhibit closed electronic shell configurations, resulting in large gaps between the highest occupied molecular orbital (HOMO) and the lowest unoccupied molecular orbital (LUMO), high ionization potentials and low electron affinities, which are shown to be a prerequisite for chemical inertness and high stability of the clusters [1–15]. In the case of alkali metal-like clusters, the magic numbers with large HOMO–LUMO gaps can be explained by the electron shell model [14]. Besides these electronic properties, compact and highly symmetric structures are often observed for magic clusters [1–15] Therefore, magic clusters are regarded as potential candidates for building blocks of new cluster materials, i.e., one may be able to synthesize cluster assemblies [16], in which original geometric structures of the free magic clusters remain unchanged. Well-known examples for magic clusters are C_{60} [1], Na_8 [5], Al_{13}^- [6,7], Sb_4 [8], Au_{20} [9], and Au_{55} [10] and some of these magic clusters are actually shown to form cluster materials [8].

Recently, attempts to synthesize new cluster materials have been extended to inorganic complexes [17]. For example, fullerene-like structures consisting of MoS_2 units were synthesized previously [18], and it was shown that $Al_{13}H$ exhibits a HOMO–LUMO gap of 1.4 eV [11]. In the present work, electronic and geometric structures of inorganic clusters consisting of 4 metallic and 6 non-metallic atoms (M_4X_6, M = W, Mo and X = O, S) are introduced. W_4O_6 clusters show a large HOMO–LUMO gap in the anion ultraviolet photoelectron spectroscopy (UPS), which is also confirmed by theoretical calculations. W_4O_6 shows a relatively low symmetry compared to other hitherto discovered magic clusters such as C_{60} and Au_{20}. Also, for W_4S_6 and Mo_4S_6, large HOMO–LUMO gaps were found using UPS, and

* Corresponding author. Fax: +49753188 3888.
E-mail address: young.kim@uni-konstanz.de (Y.D. Kim).

theoretical calculations are in line with experimental observations. Electronic structures of both isoelectric M_4O_6 and M_4S_6 are analogous, yet interestingly the geometric structure of M_4S_6 differs significantly from that of W_4O_6.

$W_4O_m^-$, $W_4S_m^-$ or $Mo_4S_m^-$ (m = *integer*, 1–6) clusters were produced by exposing W and Mo to O_2 (for oxide clusters) or H_2S (for sulphide clusters) in the pulsed arc cluster ion source (PACIS) [19]. It is important to mention that exposure of Mo to H_2S at about 600 K results in formation of MoS_2 nanostructures without H impurities [20]. The cluster temperature is sufficiently high when W and Mo react with H_2S reagents in our PACIS source, excluding the possibility that the $M_nS_m^-$ structures are contaminated by H impurities. The inorganic clusters formed in the cluster source are then cooled down in the extender, and at the UPS measurement stage, the temperature of the clusters is estimated to be room temperature. The mass of the clusters was selected by means of a time-of-flight (TOF) mass spectrometer, and the UPS spectra of the mass-selected clusters were taken using UV laser pulse (photon energy = 4.66 or 6.4 eV).

Theoretical investigations on $Mo_4S_m^-$ clusters have been performed applying the generalized gradient approximation (GGA) for the exchange-correlation potential in the density functional theory (DFT) as prescribed by Becke's three parameter hybrid functionals using the non-local correlation provided by the Lee, Yang, and Parr (commonly referred as B3LYP). The 6-311G** basis set for S and 3-21G** for Mo have been used. For $W_4O_m^-$, we used GGA for exchange-correlation potential prescribed by Becke–Perdew–Wang (commonly known as BPW91). The atomic orbitals were presented by a Gaussian basis. We used the 6-311G* basis set for O and the Stuttgart relativistic effective core potential basis set for W. The structures of both neutral and anionic clusters have been optimized globally without any symmetry constraint and by starting with various geometries. For all the calculations, GAUSSIAN 98 code has been used. Details of the calculations of the clusters will be described elsewhere [21,22].

In Fig. 1, UPS spectra of $W_4O_m^-$ for m = 0–6 are displayed. The pure W_4 cluster shows an electron affinity of 1.5 eV without any distinct indication of a HOMO–LUMO gap in the binding energy range between 0 and 6 eV. As the number of oxygen atoms attached to the tungsten host increases from 0 to 4, electron affinity increases gradually (from 1.5 to 1.9 eV). HOMO–LUMO gaps cannot be clearly discriminated in the UPS spectra for n = 0–4, whereas for $W_4O_5^-$, a single distinct peak is observed at 3.0 eV, followed by the second peak at 4.5 eV, which can be attributed to the HOMO and LUMO of the neutral cluster, respectively. Correspondingly, the HOMO–LUMO gap of the W_4O_5 cluster is determined to be 1.5 eV. For W_4O_6, the electron affinity

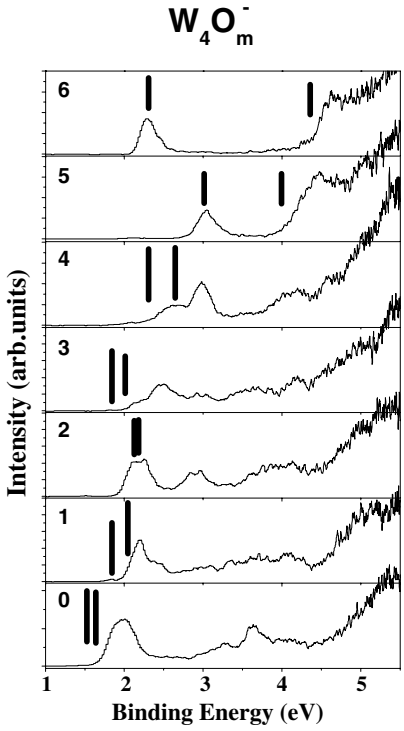

Fig. 1. UPS spectra of W_4O_m cluster anions with m = 0–6 are compared with theoretically calculated vertical detachment energies (lines in the spectra) (photon energy = 6.4 eV). The vertical detachment energies correspond to the transition energies from the anion ground states with spin state M to the neutral counterparts with $M' = M \pm 1$, which are in a geometry identical to that of the anion ground state. Good agreements between theory and experiments can be found, suggesting a high reliability of the geometric structures suggested by DFT-calculations.

becomes much lower and the HOMO–LUMO gap (2.2 eV) becomes larger compared to those of W_4O_5. Considering that a large HOMO–LUMO gap and a correspondingly low electron affinity is an indication for a closed electronic shell configuration, one can suggest that W_4O_6 clusters should exhibit a high stability and chemical inertness, and thus might be suitable for building blocks of cluster materials. The HOMO–LUMO gap cannot be distinguished in the UPS spectra, when number of oxygen atoms exceeds 7 (not shown here) [22].

To shed light on detailed geometric and electronic structures of W_4O_m clusters, theoretical calculations were performed (Fig. 2). The bare W_4 cluster shows a tetrahedral structure, which does not undergo significant relaxation with increasing number of oxygen atoms from 1 to 4. In contrast to the first four oxygen atoms, addition of the fifth oxygen atom significantly weakens the W—W bonding in the W_4 framework, resulting in insertion of two oxygen atoms in the W_4 framework to form two W—O—W bonds, thus leaving three W—W bonds. The sixth oxygen atom forms a third W—O—W bond in a W_4O_6 cluster (neutral as well as anion), leading to the formation of a hexagonal ring structure in a W_4O_6

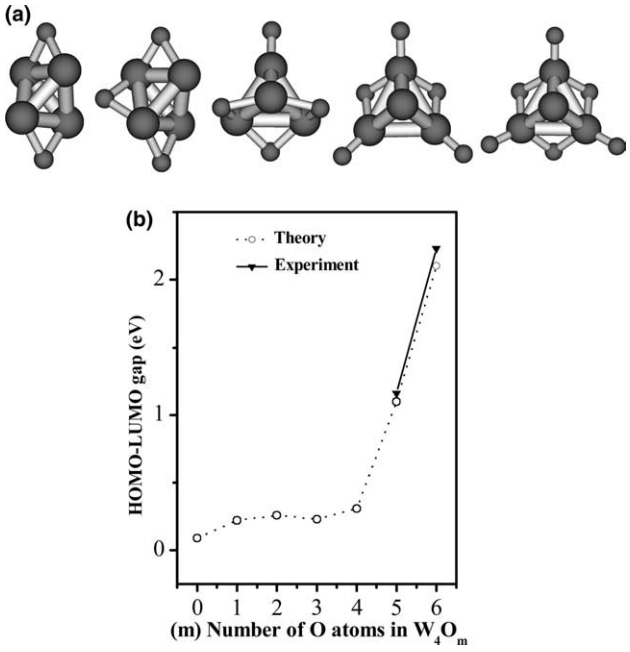

Fig. 2. (a) Optimized structures of W_4O_m with $m = 2$–6. Larger spheres correspond to W atoms, whereas smaller ones represent O. (b) The calculated HOMO–LUMO gaps are compared with experimentally determined values. For $m = 0$–4, the HOMO–LUMO gaps cannot be discriminated in the experimental UPS spectra.

cluster. The hexagonal ring structure seems to be an energetically favored arrangement of W and O atoms, since the W_3O_3 hexagonal ring was also found to be a fundamental building block of amorphous WO_3 films [23]. Therefore, it is suggestive that the tungsten oxide clusters containing this hexagonal ring is more robust than other tungsten oxide clusters without similar ring structures. In fact, a W_3O_9 cluster, which is the most abundant unit of tungsten oxide vapors (indicating that W_3O_9 is the most stable unit among various tungsten oxide clusters), also contains a hexagonal W_3O_3 ring, confirming a high stability of the W_3O_3 ring [24]. For more detailed explanations about the geometric structures of W_4O_m and their anionic counterparts, see [22].

To check the reliability of the theoretical approach used here, we have calculated the vertical detachment energies of $W_4O_m^-$ clusters. As it is displayed in Fig. 1, theoretically calculated vertical detachments energies agree with the binding energies of the peaks in the UPS spectra within 0.2 eV, confirming that the geometric structures of W_4O_m illustrated in Fig. 2 are accurate. It is important to note that the HOMO–LUMO gap of W_4O_6 is 2.2 eV, which is even larger than those of Na_8 (1.1 eV) [5], C_{60} (1.5 eV) [4], Au_{20} (1.8 eV) [9], and W@Au12 (1.6 eV) [25], implying that W_4O_6 clusters can be more stable and chemically inert than these aforementioned magic clusters.

Considering valence electronic structures, S and O are isoelectronic, as Mo and W are. Since electronic structures and chemical properties of clusters are often dominated by the number of valence electrons, one may expect W_4S_6, Mo_4O_6 and Mo_4S_6 to be magic just as W_4O_6 is. To obtain a better understanding of the structures of M_4S_m clusters, UPS spectra of $W_4S_m^-$ and $Mo_4S_m^-$ clusters were collected (Fig. 3). The general trend for the development of the UPS spectra of $W_4S_m^-$ with increasing number of S atoms (m) is analogous to that found for $W_4O_m^-$ clusters (Fig. 1). With increasing m from 1 to 5, the electron affinity gradually increases, whereas the $W_4S_6^-$ clusters show a lower electron affinity compared to that of $W_4S_5^-$. No indications for large HOMO–LUMO gaps can be observed for $W_4S_m^-$ with m = 1–5; however, the $W_4S_6^-$ cluster exhibits a distinct HOMO–LUMO gap of 1.7 eV. A similar trend can also be found for the $Mo_4S_m^-$ clusters, yielding a HOMO–LUMO gap of about 2.0 eV for Mo_4S_6 (Fig. 3). This result implies that M_4S_6 should also be extraordinarily stable and chemically inert like W_4O_6.

To get an understanding of the geometric and electronic structures of Mo_4S_m clusters, theoretical calculations were also performed. The optimized ground state structures of these clusters are shown in Fig. 4a. Analogous to W_4, Mo_4 exhibits a tetrahedral structure. In contrast to the case of W_4O_m, the geometries of Mo_4S_m clusters undergo a sudden transformation when three S atoms are attached to the Mo_4 frame, leading to the conversion of the metallic tetrahedron frame to a rectangular ring. In Mo_4S_4 the nearly tetrahedral structure of the Mo_4 unit is retained. The same holds for Mo_4S_5. Finally, all edges of the Mo_4 tetrahedron are bridged by S in the Mo_4S_6 cluster, yielding a three dimensionally compact and symmetric tetrahedral structure. The

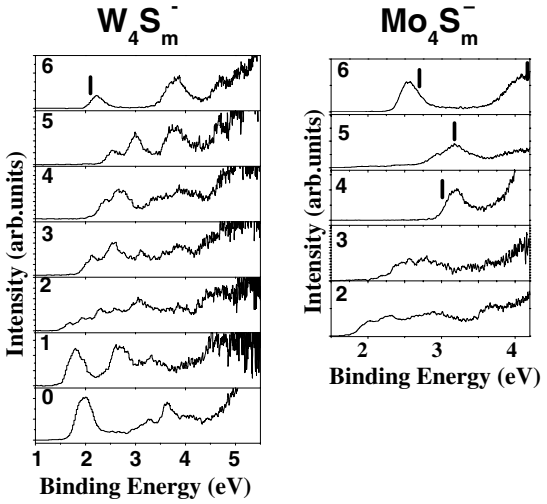

Fig. 3. UPS spectra of W_4S_m (photon energy = 6.4 eV) and Mo_4S_m (photon energy = 4.66 eV) cluster anions with $m = 0$–6 are shown. For Mo_4S_m ($4 \leqslant m \leqslant 6$) and W_4S_6 theoretically determined vertical detachment energies (lines in the spectra) are compared with experimental data.

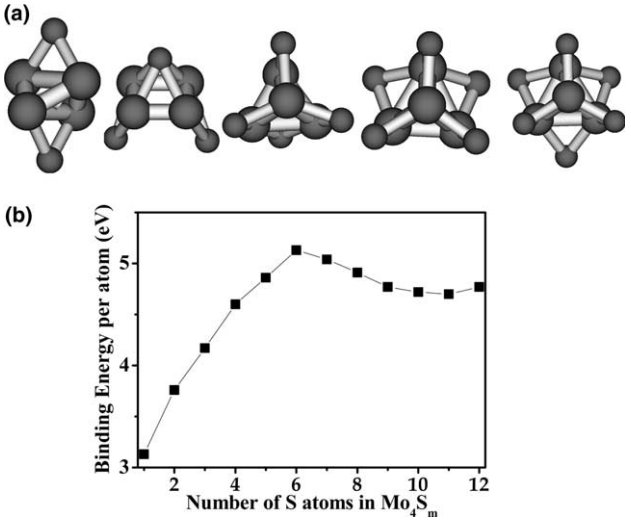

Fig. 4. (a) Optimized structures of Mo_4S_m with $m = 2$–6. (b) The calculated binding energies per atoms of Mo_4S_m with $m = 1$–12.

structure of Mo_4S_6 is much different from that of W_4O_6, which has a much lower symmetry with three terminal O atoms attached to the W_3O_3 hexagonal ring (Fig. 2). It seems that S tends to have bridge bonding with metal atoms, whereas O can form double bonds with a metal atom. Theoretically calculated vertical detachment energies are consistent with the experimental data (Fig. 3). The theoretically determined HOMO–LUMO gap of Mo_4S_6 is the largest among the Mo_4S_m clusters studied in the present work, in line with the experimental data.

In Fig. 4b, the binding energies per atom for Mo_4S_m clusters are plotted versus number of S atoms (m). The binding energy of the Mo_4S_6 cluster represents a maximum in the series Mo_4S_m ($m = 1\ldots12$), indicating that the Mo_4S_6 clusters is indeed the most stable, and therefore, most likely chemically inert.

Currently, no detailed theoretical calculations on $W_4S_m^-$ clusters exist. However, the structural similarities between MoS_2 and WS_2 in bulk form as well as in nanocomposites have been verified in previous studies, suggesting that the structural evolution of W tetramer upon addition of S may be analogous to the case of the Mo tetramer [26]. According to our preliminary theoretical calculations, the electron affinity of W_4S_6 with the same geometry as that of Mo_4S_6 amounts to 2.1 eV, which is in line with the experimental data in Fig. 3, suggesting that the geometric structure of Mo_4S_6 in Fig. 4 can be also valid for W_4S_6.

W_4O_6 and Mo_4S_6 show larger HOMO–LUMO gaps than other non-magic clusters consisting of the same elements. The electronic structures of clusters are generally sensitive to the geometric structure [9], and therefore analogous electronic structures of different clusters are often regarded as indicative of similar geometric structures, i.e., it could be tentatively suggested that these two clusters should exhibit identical structures. However, according to our detailed theoretical calculations, both clusters show different geometries, implying that the electronic structures of both clusters should be dominated by the number of valence electrons. Magic numbers of metallic clusters are generally explained by simple electron counting rules such as the one-electronic shell model for alkali and coinage metal clusters [14] or the 18-electron rule for d-metal complexes [25]. In a purely ionic model, considering that O and S act as two-electron acceptors and Mo and W atoms have 6 electrons in the valence d shells, 12 electrons are left in the M_4 frameworks of the magic M_4X_6 clusters. These 12 electrons, i.e. 2 electrons per tetrahedron edge ('bond') could be sufficient for the explanation of the bonding within the M_4 framework. Another, less ionic description, but with some reminescence to the jellium model could also explain the 'magic' character of the M_4X_6 clusters. The tetrahedral W_4/Mo_4 clusters have 24 valence electrons, corresponding to a closed jellium shell (20 electrons) plus 4 electrons left. In the case of the M_4X_6 clusters these 4 additional electrons may be donated to sulfur or oxygen, leaving the 20 electrons at the W_4/Mo_4 core of the clusters. This would correspond to formal charges of +1 and −2/3 for W/Mo and S, respectively.

In conclusion, we have shown that M_4X_6 with M = W, Mo and X = O, S show large HOMO–LUMO gaps and therefore they should be chemically inert and more stable than other non-magic clusters. These clusters can be candidates of building blocks of cluster materials. In particular, W_4O_6 has a lower symmetry than other hitherto discovered magic clusters; however, it is more 'magic' than other magic clusters in terms of electronic structure. Similar electronic structures of M_4S_6 and M_4O_6 may be regarded as an evidence for identical geometric structure of both clusters; however, our detailed DFT-calculations show that both clusters have much different geometric structures, implying that synergetic approach between theory and experiment is inevitable to completely understand cluster geometries.

Acknowledgements

N.B., G.G., Y.D.K., J.T. and G.S. are grateful for the financial support from Deutsche Forschungsgemeinschaft (DFG). Q.S. and P.J. acknowledge partial support from the Department of Energy.

References

[1] H.W. Kroto, J.R. Heath, S.C. O'Brien, R.F. Curl, R.E. Smalley, Nature (London) 318 (1985) 162.
[2] S.H. Yang, C.L. Pettuette, J. Conceicao, O. Cheshnovsky, R.E. Smalley, Chem. Phys. Lett. 139 (1987) 233.

[3] W. Krätschmer, L.D. lamb, K. Fostiropoulos, D.R. Hufman, Nature 347 (1990) 354.
[4] O. Cheshnovsky, S.H. Yang, C.L. Pettiette, M.J. Craycraft, Y. Liu, R.E. Smalley, Chem. Phys. Lett. 138 (1987) 119.
[5] H. Häkkinen, U. Landmann, Phys. Rev. Lett. 76 (1996) 1599.
[6] X.-B. Wang, L.-S. Wang, Phys. Rev. Lett. 81 (1998) 1909.
[7] J. Akola, M. Manninen, H. Häkkinen, U. Landman, X. Li, L.-S. Wang, Phys. Rev. B 60 (1999) R11297.
[8] T.M. Bernhardt, B. Stegemann, B. Kaiser, K. Rademann, Angew. Chem. Int. Ed. 42 (2003) 199.
[9] J. Li, H.-J. Zhai, L.-S Wang, Science 299 (2003) 864.
[10] H.-G. Boyen, G. Kästle, F. Weigl, B. Koslowski, C. Dietrich, P. Ziemann, J.P. Spatz, S. Riethmüller, C. Hartmann, M. Möller, G. Schmid, M.G. Garnier, P. Oelhafen, Science 297 (2002) 1533.
[11] S. Buckart, N. Blessing, B. Klipps, J. Müller, G. Ganteför, G. Seifert, Chem. Phys. Lett. 301 (1999) 546.
[12] H. Kietzmann, R. Rochow, G. Ganteför, W. Eberhardt, K. Vietze, G. Seifert, P.W. Fowler, Phys. Rev. Lett. 81 (1998) 5378.
[13] J. Müller, B. Liu, A.A. Shvartsburg, S. Ogut, J.R. Chelikovwsky, K.W.M. Siu, K.-M. Ho, G. Ganteför, Phys. Rev. Lett. 85 (2000) 1666.
[14] W.A. de Heer, Rev. Mod. Phys. 65 (1993) 611.
[15] B.K. Rao, P. Jena, S. Buckart, G. Ganteför, G. Seifert, Phys. Rev. Lett. 86 (2001) 692.
[16] S.N. Khanna, P. Jena, Phys. Rev. Lett. 69 (1992) 1664.
[17] A. Kasuya, R. Sivamohan, Y.A. Barnakov, I.M. Dmitruk, T. Nirasawa, V.R. Romanyuk, V. Kumar, S.V. Mamykin, K. Tohji, B. Jeyadevan, K. Shinoda, T. Kudo, O. Terasaki, Z. Liu, R.V. Belosludov, V. Sundararajan, Y. Kawazoe, Nat. Mat. 3 (2004) 99.
[18] L. Margulis, G. Salitra, R. Tenne, M. Talianker, Nature 365 (1993) 113.
[19] C.-Y. Cha, G. Ganteför, W. Eberhardt, Rev. Sci. Instrum. 63 (1992) 5661.
[20] S. Helveg, J.V. Lauritsen, E. Lægsgaard, I. Stensgaard, J.K. Nøslash rskov, B.S. Clausen, H. Topsøe, F. Besenbacher, Phys. Rev. Lett. 84 (2000) 951.
[21] J. Tamuliene, G. Seifert, to be published.
[22] Q. Sun, B.K. Rao, P. Jena, D. Stolcic, G. Ganteför, Y. Kawazoe, Chem. Phys. Lett. 387 (2004) 29.
[23] A. Balerna, E. Bernieri, E. Burattini, A. Kuzmin, A. Lusis, J. Purans, P. Cikmach, Nucl. Instrum. Meth. Phys. Res. A 308 (1991) 234.
[24] J. Berkowitz, W.A. Chupka, M.G. Inghram, J. Chem. Phys. 27 (1957) 85.
[25] X. Li, K. Boggavarapu, J. Li, H.J. Zhai, L.S. Wang, Angew. Chem. Int. Ed. 41 (2002) 4786.
[26] G. Seifert, H. Terrones, M. Terrones, G. Jungnickel, T. Frauenheim, Phys. Rev. Lett. 85 (2000) 146.